Acta Astronautica 211 (2023) 163–176

Contents lists available at ScienceDirect

Acta Astronautica

journal homepage: www.elsevier.com/locate/actaastro

Moon Diver: Exploring a pit's exposed strata to understand lunar volcanism ☆

Issa A.D. Nesnas [a,*], Laura Kerber [a], Glenn Sellar [a], Tibor Balint [a], Brett Denevi [b], Aaron J. Parness [c], Richard P. Kornfeld [a], Miles Smith [a], Patrick McGarey [c], Travis Brown [a], Eric Sunada [a], Kurt A. Gonter [c], Benjamin Hockman [a], Paul Hayne [d], Tyler Horvath [e], Joshua B. Hopkins [f], Andrew E. Johnson [a], Robert V. Wagner [g], Yang Cheng [a], Aaron G. Curtis [a], Kris Zacny [h], Michael Paton [a], Kristopher V. Sherrill [a]

[a] Jet Propulsion Laboratory, California Institute of Technology, 4800 Oak Grove Dr., Pasadena, CA, 91106, USA
[b] John Hopkins Applied Physics Laboratory, 11100 Johns Hopkins Rd, Laurel, MD, 20723, USA
[c] Formerly at Jet Propulsion Laboratory, California Institute of Technology, 4800 Oak Grove Dr., Pasadena, CA, 91106, USA
[d] University of Colorado Boulder, 391 UCB, 2000 Colorado Ave, Boulder, CO, 80309, Duane Physics Building, Rm. E226, USA
[e] University of California, Los Angeles, Earth, Planetary, and Space Sciences, 595 Charles E. Young Dr, Geology Room 4712, Los Angeles, CA, 90095, USA
[f] Formerly at Lockheed Martin Space, 12257 S. Wadsworth Blvd, Littleton, CO, 80128, USA
[g] Arizona State University, Lunar Reconnaissance Orbiter Camera, P.O. Box 873603, Tempe, AZ, 85287-3603, USA
[h] Honeybee Robotics, 2408 Lincoln Avenue, Altadena, CA, 91001, USA

ARTICLE INFO

Keywords:
Lunar pit exploration
Exploring exposed strata
Rappelling rover
Lunar secondary-crust evolution

ABSTRACT

Natural pits on the Moon expose deep cross-sections of the lunar maria, enabling direct investigation of the Moon's volcanic history and providing potential access to subsurface lava tubes. The Moon Diver mission concept seeks to explore the Mare Tranquillitatis pit, which exposes the largest wall of bedrock of the mare pits (~65 m). The concept is enabled by two innovative capabilities: pinpoint landing near the pit and robotic access to its near-vertical wall with an instrument package to examine the elemental chemistry, mineralogy, and morphology of these bedrock layers. Pinpoint landing uses closed-loop guidance with terrain-relative navigation (TRN), which was advanced by Perseverance landing on Mars, to deliver the lander within a 100-m ellipse. The Axel robotic explorer, which remains tethered to the lander, would egress onto the lunar surface and traverse the relatively flat terrain to the pit's funnel entrance. The lander, which is the data link to Earth, also serves as an anchor and provides power and communication to the rover through its tether. The rover is a novel two-wheeled platform with a trailing boom and a spool that pays out the tether as the rover traverses toward the pit. The 300-m long tether is well margined for the rover to scale the pit wall. The rover carries a surface preparation tool and three additional instrument types: (a) three high-resolution cameras for acquiring context images of the near and far walls with the near-wall pair in a stereoscopic configuration, (b) an alpha-particle-X-ray spectrometer (APXS) for elemental composition, and (c) a multi-spectral microscopic imager (MMI) that uses controlled lighting for mineralogy. The surface-preparation tool removes dust and patina from the rock wall by grinding a small area. This tool, the MMI, and the APXS would be deployed from an instrument bay inside the wheel wells. The rover would independently point each instrument at the same target on the wall with millimeter repeatability. Landing shortly after sunrise, the surface mission timeline is just shy of a lunar daytime (14 Earth days). Beyond the primary mission, the rover would be capable of descending from the overhang and peering into the void that may open to a large cave or lava tube. Lunar pits provide an exciting new target for exploration using innovative robotic capabilities that have been tested with integrated science instruments at multiple terrestrial analogue sites including a pit with basaltic layers in Arizona.

☆ JPL Clearance: CL#22–4534. The information presented about the Moon Diver mission concept is pre-decisional and is provided for planning and discussion purposes only. © 2023. All rights reserved.

* Corresponding author.
E-mail addresses: Issa.Nesnas@jpl.nasa.gov (I.A.D. Nesnas), Brett.Denevi@jhuapl.edu (B. Denevi), Aaron.J.Parness@gmail.com (A.J. Parness), Paul.Hayne@colorado.edu (P. Hayne), tylerhorvath@g.ucla.edu (T. Horvath), jhopkins@blueorigin.com (J.B. Hopkins), Robert.V.Wagner@asu.edu (R.V. Wagner), kazacny@honeybeerobotics.com (K. Zacny).

https://doi.org/10.1016/j.actaastro.2023.05.042
Received 28 February 2023; Received in revised form 16 May 2023; Accepted 28 May 2023
Available online 10 June 2023

Acronyms/Abbreviations

APXS	Alpha-particle X-ray Spectrometer
IMU	inertial measurement unit
LRO	Lunar Reconnaissance Orbiter
MMI	Multi-spectral Microscopic Imager
NAX	Narrow-Angle Camera
PCM	Phase Change Material
SPT	Surface Preparation Tool
TRN	Terrain-relative navigation

1. Introduction

During the early period of planetary differentiation, the surface of the Moon cooled, forming its primary crust. Sequences of lava layers were extruded from its deep interior, forming its secondary crust. These events cemented a record from this early differentiation period, retaining information from both the primary and secondary crusts and providing a window into the Moon's internal structure. The crusts are well preserved since the Moon is subject to few confounding geological processes such as water, wind, and plate tectonics [1]. When compared to Mars, Venus, Mercury, or Vesta [2–5], the lunar surface is also relatively more accessible. However, in most places on the Moon, a thick blanket of regolith obscures the secondary crustal bedrock from view.

The recent discovery of lunar pits opened a natural portal to allow us to peer into the lunar interior by examining exposed strata. First detected by JAXA's SELENE/Kaguya mission [6] and subsequently observed by NASA's Lunar Reconnaissance Orbiter (LRO) [7,8], the pits revealed tens of meters of pristine, bedrock stratigraphy, offering a unique opportunity to directly access the basaltic layers. The samples collected by the Apollo astronauts provided an unprecedented window into the processes that shaped the Moon, serving as a "keystone" for understanding planetary geological processes throughout the solar system. But unlike these regolith-derived samples—which are like scattered puzzle pieces—the examination of the lunar pit wall would provide the missing context for their formation that would help us understand the bigger picture of how the Moon's crust was formed.

The goal of the Moon Diver mission concept is to better understand the fundamental processes of secondary crust differentiation and formation by studying the origins, emplacement processes, and evolution of the Moon's secondary crust (the lunar maria). It does so by accessing and collecting elemental chemistry, mineralogy, and morphology measurements of regolith and bedrock layers of the pit wall. This would allow us to investigate where rocky crusts come from, how they are emplaced, and the process by which they are transformed into the regolith layer that we see from space. In doing so, the mission would combine the deep knowledge gained by Apollo with the unprecedented *in-situ* access to secondary crust granted by the lunar mare pit to understand these fundamental processes on the Moon.

Conducting a scientific investigation in lunar pits presents three key challenges. The first is accessing the pit wall, which requires landing at a safe but close distance to the pit in the region of the exposed wall that would be explored, traversing hazardous topography to reach and scale the wall, and deploying multiple instruments on the wall's irregular surfaces. The second challenge is the thermal environment that concentrates heat on the lit wall due to the concave geometry of the pit. The third is conducting the surface mission with an explorer that is occluded from its communication relay.

Two key capabilities enable the Moon Diver mission concept to acquire measurements across the pit wall. The first is pinpoint landing, which delivers the science payload in the vicinity of the pit and within a margined 100 m landing ellipse. The second is extreme-terrain mobility with a capability to scale steep slopes including vertical walls and overhangs (Fig. 1). The platform leverages its mobility to deploy multiple instruments. Designed for low mass and minimal actuation, the rover uses the same actuators for both mobility and instrument placement. The low-power rover minimizes heat dissipation and uses operational constraints to avoid the highest temperatures around lunar noon. The mobility system would deliver and deploy multiple instruments onto the pit wall to acquire measurements. Measurements are relayed to the lander via the umbilical tether and subsequently delivered to the ground operations team.

The concept of operations spans a 14 Earth-day mission, with landing scheduled shortly after sunrise. Following that, the rover would egress from the lander, traverse toward the pit, descend along the pit funnel and rappel down its wall. Throughout its traverse, the rover would acquire numerous measurements of both regolith and mare layers. After descending to the bottom of the layers, the rover would reach a significant overhang (Fig. 2). This void space may open into a large cave or lava tube, which could someday provide a protected location for a lunar base. For these reasons, lunar pits provide an exciting new target for lunar exploration.

The Moon Diver mission concept was proposed to the NASA 2019 Discovery opportunity. The rover design is based on the fielded JPL Axel rover design and adapted for the lunar environment. The lander design is from Lockheed Martin and is based on the successful Mars Phoenix and InSight landers and the designs developed for the MoonRise lunar lander proposed to New Frontiers [10].

2. Science motivation

2.1. Why lunar pits?

Lunar pits are ideal for accessing stratigraphic layers because they form via collapse, which preserves the morphology of the layers without perturbing them [8]. While other locations, such as large crater walls, have also revealed layering, such layers have been subjected to impact, which may shock, break, or at times invert the layers.

2.2. Why Mare Tranquillitatis?

Located at 8.335° N, 33.222° E, the Mare Tranquillitatis pit (Fig. 3) is particularly compelling among the 16 known lunar pits in the maria because it exposes one of the largest vertical extents of layers among the mare pits. Furthermore, it is critically located on the boundary between two distinct Tranquillitatis lava types and it sits above one of the largest confirmed void spaces. The pit has a diameter that ranges from 88 to 100 m, a depth of approximately 133 m [11], and a wall height of 80–90 m (see Fig. 4). Identifying the lava layers in context across the pit wall and correlating them to the two lava types and samples collected by Apollo astronauts [12] allows us to leverage 50 years' worth of sample analyses.

Lunar mare pits may open into deep subsurface void spaces or lava tubes. The bottom of the Tranquillitatis pit opens onto a void that extends back a minimum of 25 m [8]. In addition to their scientific interest, lunar caves could be of interest for future habitation as they naturally protect from radiation, micrometeorites, and temperature swings [13]. The Moon Diver mission would enable us to peer into the void and assess the feasibility of such an architecture. In this way, Moon Diver helps us understand the Moon's past while preparing for its future.

2.3. Modelling the pit

The descent path of the rover is determined by the actual landing location since the rover follows a straight-line path into the pit. The

relatively flat and hazard-free terrain surrounding the pit offers multiple viable locations for placing the landing ellipse. Among the landable regions, some offer advantages in terms of thermal conditions, lighting, and wall-contact. One such candidate safe landing site lies northwest of the pit, which provides favorable access to multiple sections with afternoon shadow for a cooler excursion but sufficient light for sensing based on a thermal and light analyses of the modeled pit that we conducted.

2.3.1. Topography

Using the highest resolution images of the Mare Tranquillitatis available at this time—at 0.5 m/pixel from LRO's Narrow-Angle Camera (NAC) [7]—we used precision mapping techniques to reconstruct the 3D topography [14,15]. Images acquired from multiple viewpoints and sun angles were also crossmatched to the Lunar Orbiter Laser Altimeter (LOLA) data for global registration to estimate slope information relative to gravity vector (Fig. 5 (top)). We analyzed cross sections of the reconstructed wall based on multiple landing sites to understand regions that maximize wall contact for *in-situ* measurements (Fig. 6). When the rover separates from the wall by a few meters (across the overhung regions), it acquires remote measurements including stereoscopic context imaging. This assessment shows sufficient contact with the multiple wall layers for the required contact measurements, though refinements of the pit wall geometry is ongoing [11,16] .

2.3.2. Thermal

Given the low resolution of available thermal data at this time—at 200 m/pixel from LRO's Diviner Lunar Radiometer Experiment—we relied on models of the reconstructed 3D topography to develop detailed thermal models, since variations in temperature around the pit are complex. With an east-west Sun trajectory at an ~8° inclination, the south-most wall is permanently shadowed and both the north and south walls have more tempered rise/fall temperatures with peaks 25–40 K lower than the east and west walls. While this makes the north/south walls more favorable targets, the limited imagery (none of the south wall and a few of the north) and topographic data makes planning for these walls more difficult. Temperatures of the surface surrounding the pit reach ~385 K, while the pit wall and floor can reach ~410 K. With an early lunar morning landing and with time required to commission, egress, and traverse to the pit while conducting science, the west wall would be more favorable for an afternoon pit excursion, being the shadowed wall (Fig. 5 (bottom)). Any contingency or delay in reaching the pit wall will continue to reduce the peak temperatures on the wall. Other benefits to landing west of the pit and driving eastwards toward the west wall include avoiding self-shadows that remain behind the rover as it approaches the pit. As more orbital imagery of the north wall becomes available from LRO, that will further relax the thermal requirements and open up approaches from the north of the pit. Understanding of the thermal environment of the pit continues to advance significantly through modeling [17].

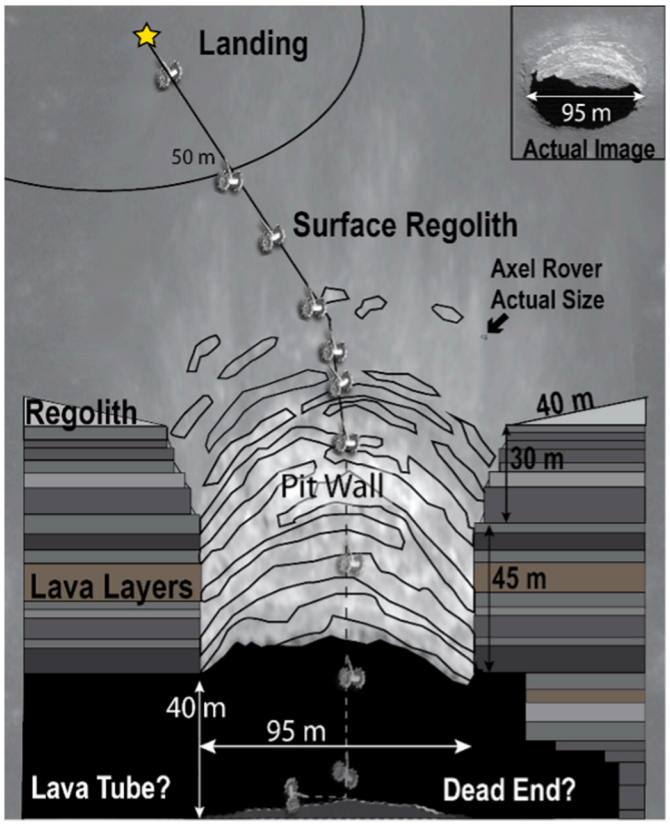

Fig. 2. A schematic cross-section of the pit. On all sides of the pit, there are accessible stair-step layers in the funnel down to 30–33 m depth. Some walls are potentially accessible down to ~80 m depth. At the bottom of the pit, there is a large void, which could be a lava tube.

3. Science goals, objectives, and measurements

3.1. Goals and objectives

The Moon Diver mission concept has the following three goals:

Goal 1: Interior Composition: understand the differentiation of terrestrial planetary bodies by constraining the source regions of the Moon's titanium-rich lavas. Towards the end of the Moon's differentiation, a titanium-rich layer would have formed between the mantle and the crust. The extent to which this layer later mixed into the mantle during a whole-mantle overturn is an outstanding question in lunar science [18]. The location of the Tranquillitatis pit at the juncture of two lavas with differing amounts of titanium allows us to investigate this question The specific objective is to *determine depth of the origin of the source of the mare basalts at Tranquillitatis*. By examining the nature and distribution of phenocrysts across the cross-section of the lava layers, as

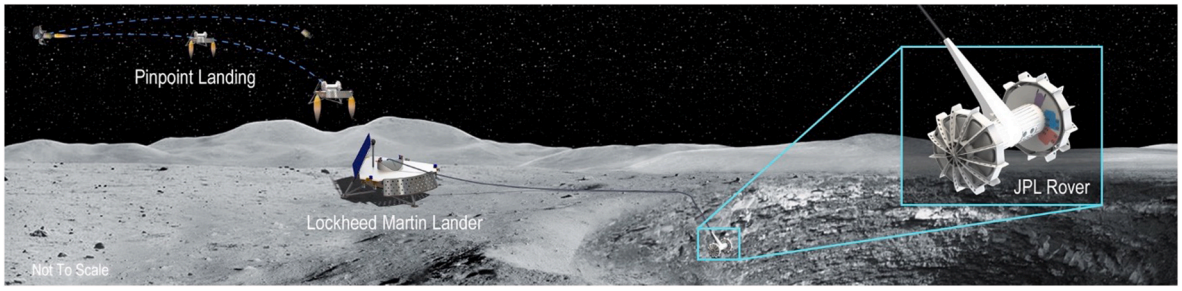

Fig. 1. The Moon Diver mission concept delivers a lander in the vicinity of the Mare Tranquillitatis pit and deploys a tethered rappelling rover with its instrument suite across the pit funnel and wall to acquire science measurements.

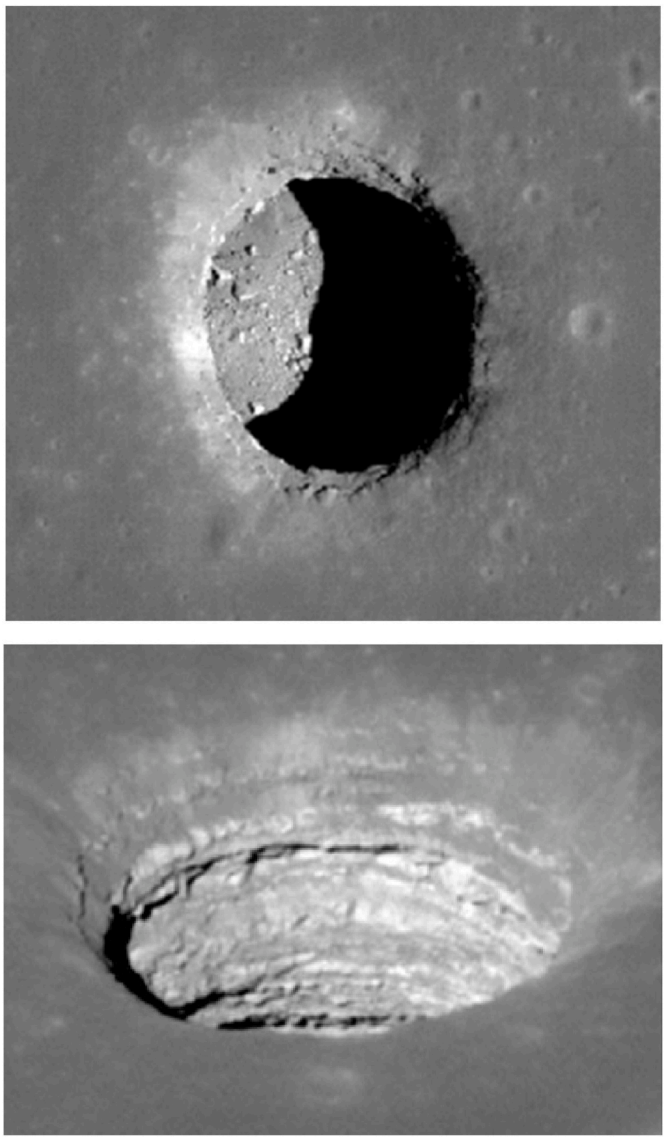

Fig. 3. The mare tranquillitatis pit credit: NASA LRO NAC (top) M126710873R (0.5 m/pix) (bottom) M144395745L [9].

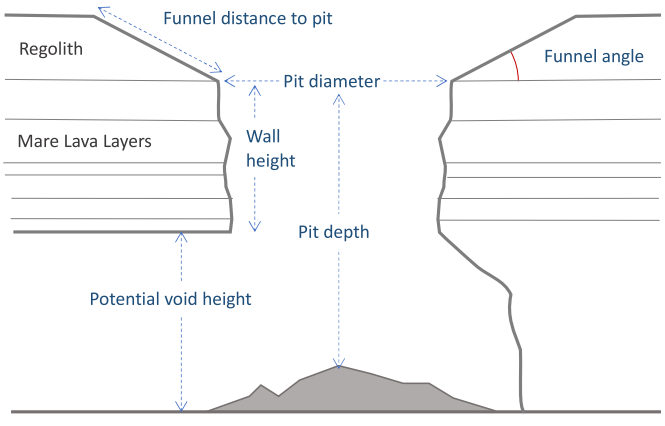

Fig. 4. Labels for pit dimensions.

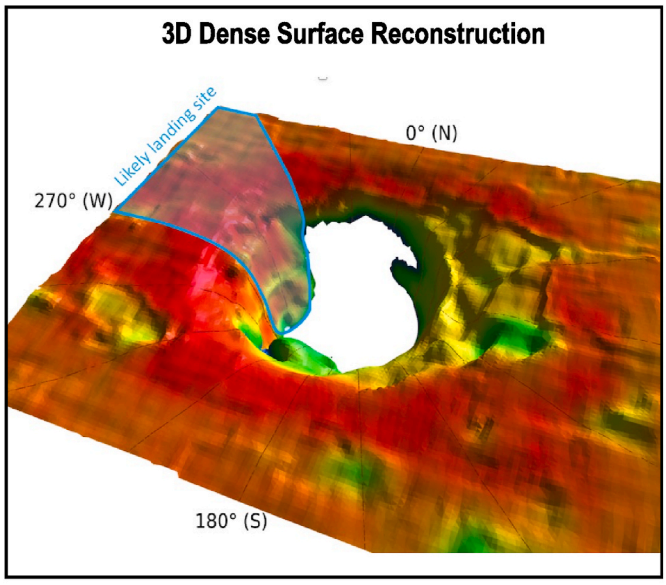

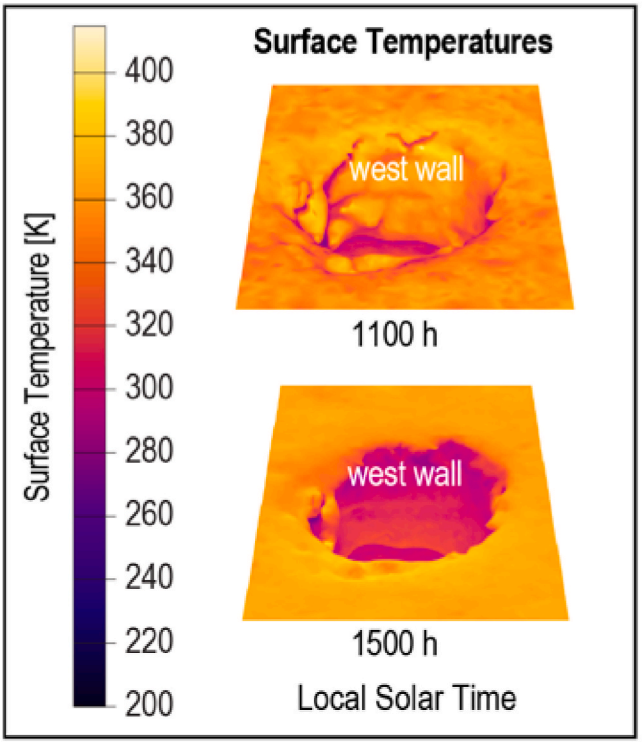

Fig. 5. 3D reconstruction of pit wall using dense feature matching (top). Targeting the west wall allows cooler temperatures for the lunar afternoon investigation.

well as the abundance of key elements, one can separate the influences of its three stages: generation, ascent, and eruption [2,19].

Goal 2: Emplacement Process: understand the emplacement regime of a planetary flood basalt. The specific objective is *to determine whether basalts were emplaced* ***catastrophically*** *in thick, turbulent flows or* ***incrementally*** *in smaller but more numerous inflated flows*. Flood basalts are voluminous outpourings of low viscosity lavas that form vast flat plains. Flood basalts, which occur in short geological periods, are the primary way that planetary bodies are resurfaced (by area) and their gas effusion can have a profound effect on the planet's atmosphere. However, because of the lack of cross-sectional data for other planets, the effusion rate of extra-terrestrial basalts remains unknown to many orders of magnitude, and their effects on their ancient atmospheres remain

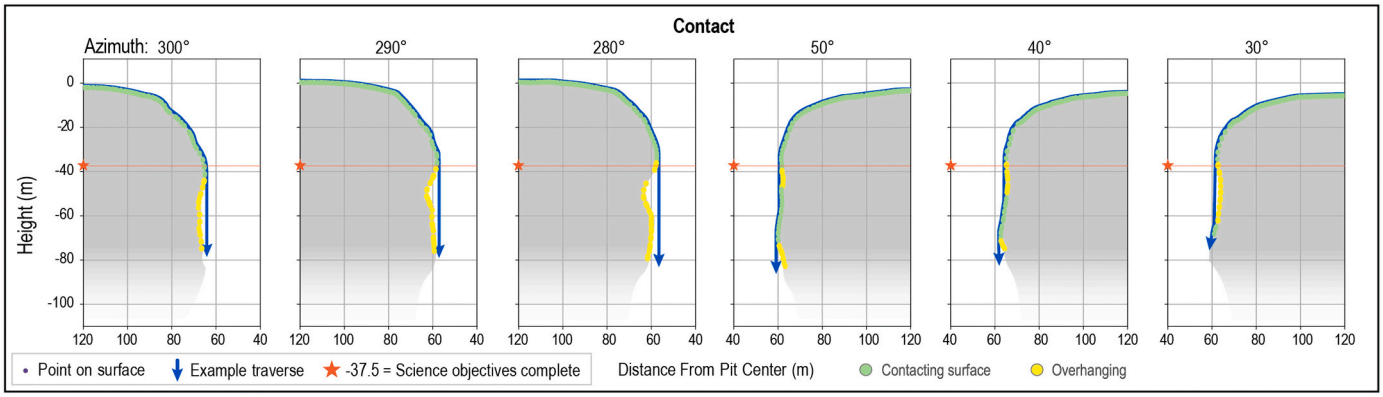

Fig. 6. Cross section of the reconstructed east and west walls of Mare Tranquillitatis (bottom) (0° points North) showing sufficient surface contact at multiple transects.

difficult to estimate [20,21]. Fundamental knowledge gained by studying the well-preserved flood basalts of Mare Tranquillitatis on the Moon would advance our knowledge and understanding of the process of flood basalts emplacement throughout the solar system.

Goal 3: Regolith Formation: understand how regolith develops from rock on an airless body. There are two objectives to meet this goal*: (1) determine the extent to which the regolith is representative of the underlying bedrock as opposed to exogenous or allochthonous components and (2) determine the nature of the transition from regolith to bedrock*. Measuring differences in composition and grain size across the depth of the regolith to its interface with the underlying bedrock advances our understanding of the models of lunar regolith formation and provides a keystone for understanding regolith processes on other airless bodies such as Mercury, asteroids, and many outer solar system moons.

3.2. Measurements

For ***Goal 1*** "*determine the depth of the source of the mare basalts at Tranquillitatis,*" three types of measurements are required: (1) images of the basalts, showing whether they are glassy or crystalline, and how the basalts vary from top to bottom (i.e., the missing context); (2) a measurement of the mineralogy of the basalts, which tells us about the temperature and pressure conditions present during their ascent; and (3) a measurement of the elemental chemistry of the basalts, including how lavas layers in the section are related to one another.

For ***Goal 2*** "*determine whether basalts were emplaced* ***catastrophically*** *in turbulent flows or* ***incrementally*** *in smaller but more numerous inflated flows,*" eight measurements are required: (1) the elemental and (2) mineralogical composition of the basalts, as above (to estimate their density and rheology); (3) images of their vesicle and crystal distributions (which also affects their viscosity), (4) images of the lavas from a distant vantage point to measure their thicknesses; (5) images used to distinguish their flow morphologies (which are proxies for their effusion rates); (6) small-scale flow textures, (7) rheological indicators (e.g., sheared vesicles), and lastly, (8) the presence or absence of paleo-regolith layers, which would indicate a long hiatus in lava effusion.

For ***Goal 3***, "*determine the extent to which the regolith is representative of the underlying bedrock*" and "*determine the nature of the transition,*" five measurements are required: (1) the chemical and (2) mineralogical composition of the regolith vs. depth and comparison to the underlying basalts, (3) the presence and frequency of layers and the approximate size distribution in the grains that compose them, (4) the frequency of large grains and rocks mixed into the regolith with depth; and finally, (5) the frequency and orientation of fractures in the basalts (all provided by micro and context imaging).

4. Instrument payload

All these measurements can be achieved with a surface preparation tool and three instrument types: (1) context cameras for near- and far-field viewing, (2) a multispectral micro-imager (MMI) for mineralogy, and (3) an alpha-particle X-ray spectrometer (APXS) for elemental composition.

4.1. Surface preparation tool

The surface preparation tool serves three purposes: (1) to clear the dust from the target surface to disambiguate the chemical composition and mineralogy of the target lava layer from that of the deposited regolith dust; (2) to grind the rocky surface to remove any microscopically thin impact glass patina that may be present; and (3) to flatten a small surface area for the MMI and APXS instrument placement. A prototype of SPT was developed by Honeybee Robotics (see Fig. 7).

4.2. Context cameras

The three context cameras serve both science and engineering purposes. For science, they would help understand the geomorphology of the lavas and provide context imagery needed to choose targets for the contact instruments. For engineering, they help perceive the environment to create 3D topographic maps, assess terrain for mobility, and help guide the rover from the ground.

The cameras use identical high resolution visual imagers with two lens types: (a) wide field-of-view (WFOV) lenses used by the stereoscopic cameras for near-field viewing of the terrain and pit wall and a narrow field-of-view (NFOV) lens on the monocular imager for viewing the far wall. The baseline context imagers are the Enhanced Engineering Cameras (EECAMs) that are successfully used on the Perseverance rover [22]. Backup alternatives, such as Redwire's high resolution cameras planned for use in human-space flight, are also available. The cameras will be pointed using the rover mechanism.

The near-field stereo cameras provide a resolution of ~0.1 mm/pixel for the determination of lava types and to identify priority measurement spots for the other instruments. The NFOV camera images the far wall of the pit at a resolution of 3 cm/pixel to count the number of lava layers and measure their corresponding thicknesses.

4.3. Alpha-particle X-ray spectrometer

The purpose of the APXS is to measure the abundances of the major and some minor elements: for example, Mg, Al, Si, K, Ca, Ti, Cr, Mn, Fe, Ni. On Mars, APXS has also measured Na, P, S, Cl, Mn, Zn, Br, Rb, Sr, Y [23]. The APXS is a mature contact instrument that has flown in different forms on four Mars missions [24] (see Fig. 8). By irradiating a

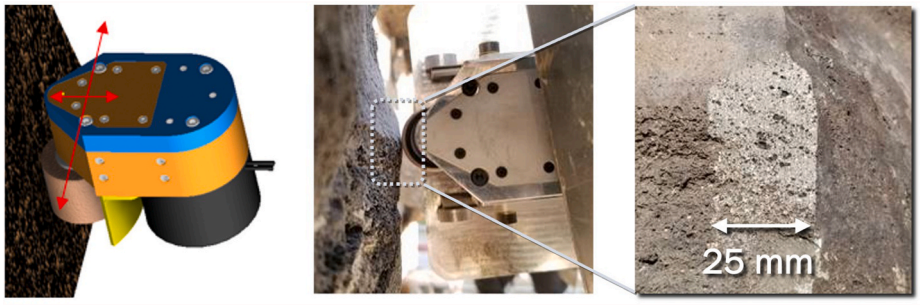

Fig. 7. Surface preparation tool design (left), prototype (middle), and result from grinding a basaltic rock on a vertical wall (right).

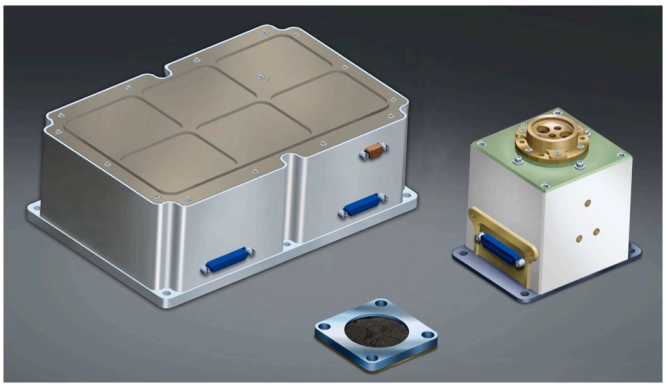

Fig. 8. The Alpha-Particle X-ray Spectrometer electronics box (left), measurement head (right), and calibration target (bottom) [23].

1.7 cm diameter spot with X-rays and alpha particles from its Cm^{244} source, it induces X-ray and alpha particles emissions that allow the quantification of specific elements. Integration-time ranges from 10 min to approximately 3 h, depending on the signal-to-noise ratio required for an individual measurement [25]. The version of APXS designed for Moon Diver, which includes a modern detector, can acquire most of the required measurements in 10 min, with an integration time of no more than 1 h for in-depth analysis of special targets. The bulk composition of the surface of a target can be inferred from APXS energy spectra.

4.4. Multispectral microscopic imager

The MMI serves a dual purpose as a microscope and a multispectral imager [26–28] (see Fig. 9). With a resolution of 18 μm/pixel, it can spatially resolve small-scale crystals, vesicles, flow features, and regolith particles and spectrally resolve mineral signatures. These include pyroclastic beads, agglutinates, and phenocrysts. To identify minerals, the instrument sequentially activates a suite of Light Emitting Diodes (LEDs) from 0.43 to 2.34 μm and records the reflectance of the surface with a broadband mercury cadmium telluride detector. The microscopic imager uses a shroud to minimize ambient light.

Table 1 shows the mass, peak power, and thermal requirements for these instruments in operations and storage modes. It compares the total to the available accommodations offered by the rover.

5. Enabling capabilities

Two key capabilities enable the Moon Diver mission concept: (1) pinpoint landing and (2) tethered rappelling mobility that can egress from the lander, traverse to the pit funnel, and descend along the pit wall on terrain whose slope could exceed vertical.

5.1. Pinpoint landing

Moon Diver delivers the lunar lander with its science-instrumented rover on a 130-day low-energy trajectory to the Moon. The trajectory is designed to deliver the lander from a north-south trajectory with an early lunar morning arrival to maximize the lunar daylight hours for the surface mission, while at the same time allowing for sufficiently

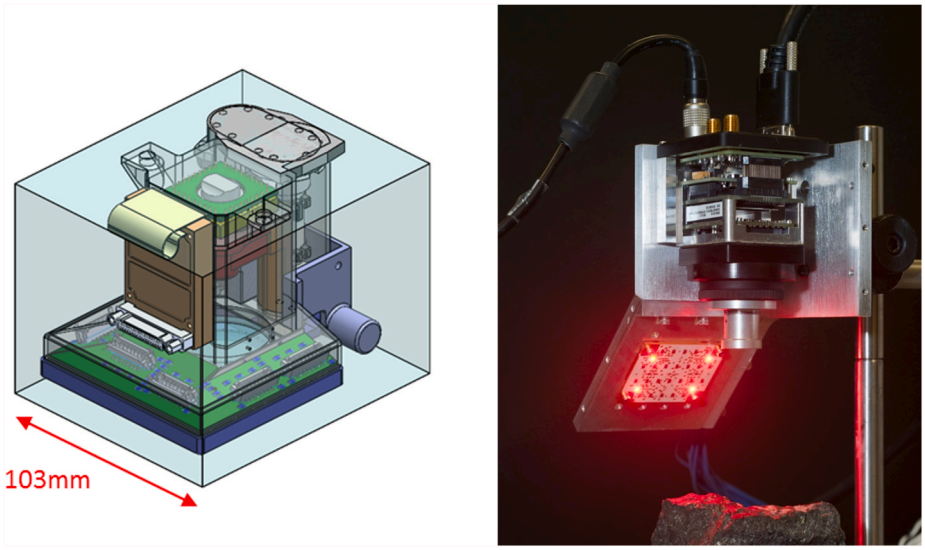

Fig. 9. The multi-spectral microscopic imager.

Table 1
The rover accommodates the cameras in the body and the SPT, MMI, and APXS in the payload bays.

	Instrument	Mass (kg)	Peak Power (W)	Thermal Operation °C[1]		Thermal Non-operation °C[2]	
Rover Body	**Rover Body Thermal Environment**			**30**	**45**	**-35**	**45**
	Cameras	**1.49**	**5.0**				
	WFOV Camera (2×)	0.69	2.5	-55	50	-128	70
	WFOV Lens (2×)	0.36	-	-110	60	-128	70
	NFOV Camera	0.35	2.5	-55	50	-128	70
	NFOV Lens	0.09	-	-90	50	-128	70
Payload Bays	**Payload Bays Thermal Environment**			**30**	**45**	**-35**	**45**
	SPT	**1.48**	**19.5**	-55	50	-128	70
	MMI	**3.74**	**27.0**				
	Head	1.10	2.8	-55	50	-128	70
	Cryocooler	0.50	15.0	-40	70	-56	80
	Calibration target	0.06	-	-128	100	-128	100
	Electronics (DPU)	2.08	12.0	-55	50	-55	70
	APXS	**1.72**	**9.0**				
	Head	0.38	0.6	*-4**	*-10**	-128	65
	Calibration target	0.12	-	-128	100	-128	100
	Electronics	1.22	8.4	-55	50	-128	70
	Total Required	**8.43**	**29.6**				
	Accommodation	**13.20**	**50**				

[1] doors open
[2] doors closed
* with closed-loop cryocooler (-35°C – -30°C)

favorable illumination of the landing site during landing. Following a final correction maneuver a few days before arrival, the lander approaches at a near horizontal flight-path angle relative to the lunar surface.

The Moon Diver mission requires pinpoint landing at a pre-selected target landing site adjacent to the pit in order to enable access by a rover that remains tethered to the lander. As such, the center of the landing ellipse is placed at the closest safe distance from the pit funnel and in the region that allows the rover to traverse a straight line to the targeted exposed wall.

To accommodate the lander approach path and allow for concurrent imaging, two cameras are used, one downward facing and a second mounted at an oblique angle. Once the lander passes the lunar arrival point, the landing sequence is executed autonomously onboard the spacecraft. The solid rocket motor is ignited to decelerate and reduce the horizontal velocity. Following the solid rocket motor burnout, the motor is jettisoned and the lander performs a separation burn. Using a combination of inertial propagation and terrain-relative navigation (TRN) measurements, the lander performs a trim maneuver to minimize downrange error that result from solid rocket performance dispersions. The latter is followed by a coast phase at the end of which the lander reorients and starts its terminal descent phase. Using a combination of TRN, altimetry and velocimetry measurements, together with onboard guidance, the lander continues to adjust its thruster, firings to reach a low terminal vertical velocity. For the next tens of seconds, the lander descends at this constant vertical velocity, and upon sensing the ground, shuts down the descent engines. Crushables in the three lander legs absorb the residual landing impact.

To enable precise landing to within 100 m ellipse, the lander uses terrain-relative navigation (TRN), providing position and velocity information during descent. Using TRN, the lander compares images taken during the landing sequence with maps of the landing site stored onboard (constructed from images taken by orbiting assets such as LRO) to establish its current position and chart a course to the landing site. This vision system repeatedly matches visual features in images acquired from its cameras to the existing terrain map. The technologies to accomplish TRN for pinpoint landing on the Moon have been in development and testing for several years and have now been validated on the Mars 2020 mission that landed the Perseverance rover [29].

5.2. *Extreme terrain mobility*

Once on the surface, and after checkouts on the lander, the rover egresses to the surface. The lander serves as the mechanical anchor for the rover, supplies it with power, and serves as a communication relay between the rover and the ground [30]. The lander, weighing much more than the rover, provides a stable anchor for rappelling. Both landing ellipse and tether length exceed the requirement by a factor of two. Through redundant conductors in the tether, the lander powers the rover and relays its commands, data, and telemetry. The tether unspools from the rover, not the lander, to prevent dragging on the surface during the traverse.

The rover carries all the instruments in dust-sealed bays. It can stop at any location and deploy the instruments in sequence on the same target. Round-the-clock shifts operate the rover in near real time, using downlinked data rather than predictions, thus simplifying operations. The 320-h surface timeline has 100% contingency allocated to science plus an additional 70% unallocated timeline margin.

Table 2 summarizes key resources on the lander and rover and shows that most resources have a large margin when compared to what the mission requires.

6. Surface mission

6.1. *The Axel rover*

Moon Diver uses the extreme-terrain Axel rover for its surface mission [32]. Axel is a two-wheeled tethered rover that is anchored to the lander via a tether (see Fig. 12). It carries hundreds of meters of tether that it pays out as the rover traverses away from the lander. With the aid of the tether, the rover can rappel down steep slopes and descend overhangs [33]. The rover is also capable of precisely pointing multiple instruments at a selected target. Instruments are accommodated inside Axel's body (all three cameras) or inside two large instrument bays

Table 2
Moon Diver is designed with ample margins.

	Resource	Units	CBE	Contingency	MEV	MPV	Margin
Lander	Landed power w/ Axel (worst mode)	W	127	25%	159	314	98%
	Battery capacity[1]	Ah	5.9	17%	6.9	9.8	42%
	Data storage (Axel data)	Gbit	-	-	20	51	155%
	Data rate (downlink)	kbps	-	-	384	768	100%
Axel	Mass[2]	kg	122.8	22%	150.0	190.0	27%
	Power to interface box	W	48	33%	64	Margin on lander	
	Battery peak power	W	100	50%	150	1,120	647%
	Battery capacity[1]	Ah	0.8	50%	1.2	8.8	633%
	Mass of melted PCM3	kg	1.05	43%	1.5	3.0	100%
	Total tethered distance	m	124	42%	176	300	70%
	Data storage	Gbit	-	-	17	64	276%
	Data rate (to lander)	kbps	-	-	290	2000	590%
Op	Surface ops timeline	hours	104	81%*	188	320	70%

CBE = Current Best Estimate
MEV = Maximum Expected Value
Contingency = (MEV−CBE)/CBE
Margin = (MPV−MEV)/MEV
MPV = Maximum Possible Value or Allocation (i.e., Requirement)

[1] to 70% depth of discharge limit & derated
[2] includes rover, interface box, instruments, and rover accommodations.
* a combination of 100% science & 57% engineering contingency

covered by the wheels. Each instrument bay can house three to four instruments (APXS, MMI, SPT) (see Fig. 10).

The Axel rover uses four identical actuators with aligned rotation axes to rove and point the instruments. One actuator rotates each wheel, a third rotates the boom, and a fourth rotates the spool [32]. This enables the rover to stop at any location and point the instruments at the same target.

6.1.1. Mobility

Axel drives conventionally on flat ground and its large grousers assist in rocky terrain [34]. On steep slopes, vertical cliffs, and overhangs, Axel uses its tether to rappel. The tether unspools from the rover (not the lander) to prevent it from dragging on the surface. This enables the rover to winch itself back up, like a yoyo. The rover follows a relatively straight path to the pit, circumnavigating obstacles if necessary. The rover also descends along a straight path to minimize lateral tether forces. During the descent into the funnel and pit, the tether remains taut to main control of the descent, whether Axel is in contact with the terrain or encounters a small overhang. In the unlikely case the rover tips over, or if the rover spins while descending an overhang, Axel's symmetric design allows it to operate inverted. Based on preliminary modeling, depending on the length of the overhang, spinning will get dampened in minutes from tether stiffness and its contact with the wall. Axel can operate from an inverted position by reversing the motion of its actuators. If the rover body high-centers on a rocky outcrop, body mounted grousers provide traction to roll off the high point.

During its traverse to the pit, the rover maintains its direction through onboard visual-inertial pose estimation and adjustments aided by ground operators. Visual pose estimations, known as visual odometry, matches terrain features in consecutive frames to estimate the change in rover pose between steps. Integrating gyro motions allows for tracking rover attitude changes. The combination of the two provides an integrated estimate of the rover's delta motion. Given the short distance, the drift from this incremental pose estimation is within the limits of uncertainties anticipated for the excursion.

6.1.2. Instrument pointing and deployment

By coordinating the four primary actuators (the two wheels, the boom, and the spool), the rover points its instruments, while supported by the tether (see Fig. 13). Pointing cameras and instruments on a slope does not move the wheels relative the surface nor the boom relative to the tether (even though the wheel, spool, and boom actuators all rotate). Rather such a maneuver re-orients the body, clocking multiple instruments on a selected target with excellent accuracy and repeatability (Fig. 11). To perform contact science, instruments can be deployed up to 7.5 cm below the wheel using a 4-bar mechanism. This reach together with Axel's ability to reorient its body generate a sweeping motion that allows the surface preparation tool to not only remove the patina but also flatten a small, 3.5 cm × 3.5 cm, area to accommodate the uneven topography in both directions (Fig. 7).

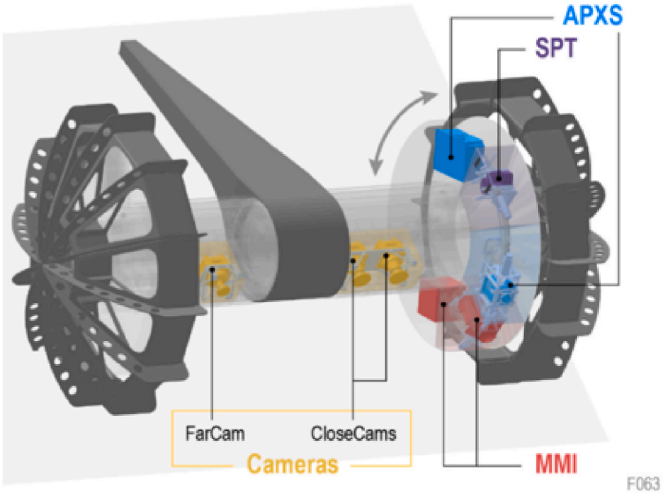

Fig. 10. The Axel rover carries the Moon Diver science payload: cameras, SPT, MMI, and APXS. Instruments are pointed by rotation of the rover body (transparent) while the wheels and boom (dark gray) remain stationary.

6.1.3. Thermal design

Axel's operation in the pit funnel and inside the pit during the morning hours represents the thermal bounding case. The most thermally stressing scenario would be an hour-long integration of the APXS on the directly illuminated side of the pit. Accordingly, the thermal system was designed to maximize heat rejection when operating the APXS on the westward facing (illuminated) part of the funnel at 10:00 LST. To maintain the desired low operational temperature for the instrument measurements, Axel uses two heritage cryocoolers, one for the APXS and a second for the MMI. For the APXS, the cryocooler maintains an APXS-rover interface at 238 K. For the MMI, the cryocooler cools the focal plane array to 170 K for its operation.

Axel uses a single thermal enclosure to house the instruments, avionics, battery, and actuators. The enclosure is designed to handle the worst case measurement scenario with sufficient margin to maintain an internal temperature within the limits of −30 °C – +50 °C. It uses multilayer insulation and segmented radiators with parabolic reflectors (Fig. 15). Two of the segmented radiators are fixed to the body while two more, connected by straps, are mounted on articulated covers that protect all radiator surfaces from lunar dust during landing and rover motions. Covers also remain closed when the sun would directly shine on the radiators during a measurement. The rover carries a thermal mass of 3 kg in the form of n-Docosane phase-change material (PCM) to hold the rover at 45 °C. Both the radiators and PCM have flight heritage from the M^3 [35] and MESSENGER flight systems respectively [36].

During the peak hot lunar hours, and if necessary, depending on the rover location, the rover performs a thermal pause, pointing the radiators at the cold sky, opening the covers, then transitioning to a low power mode while the PCM refreezes. With knowledge of lunar time, gravity vector, and slope, ground operations tools use thermal models to determine the angle to point the radiators. Analyses of possible rover and sun positions confirm that, even in the pit, the rover always has sufficient cold sky available to radiate to. The rover points the body-mounted radiators using IMU and wheel rotation feedback.

6.1.4. The tether

The tether provides mechanical support, power and communication from the lander to the Axel. Its design includes an inner core for structural integrity, an outer layer of helically wound insulated copper wires, a strength member surrounding the conductors, an abrasion layer to protect the tether from the abrasive rocks and regolith and a finish to provide ultra-violet exposure protection. There are eight wires in the tether for full redundancy for both power and communication to ensure continued operation when one or more conductors fail. The solar-powered lander provides power to trickle charge batteries inside the Axel through the umbilical tether throughout the surface mission.

Several tether prototypes have been developed and characterized for their mechanical, electrical, and environmental properties [38]. Fig. 16 summarizes results from mechanical, electrical, and environmental testing of the well margined tether that include characterizing static and dynamic load capability, bending capability, and abrasion resistance, in particular, on sharp basaltic lava and ultra-fine angular regolith under maximum load. Because the tensile strength has a 20 × margin under lunar gravity conditions, the same tether is used for Earth based testing (see Fig. 17).

In the Moon Diver mission concept, there is no requirement to return the rover to the lander, so the tether will largely be paid out without large rewinding on the spool. As such, a complete tether management

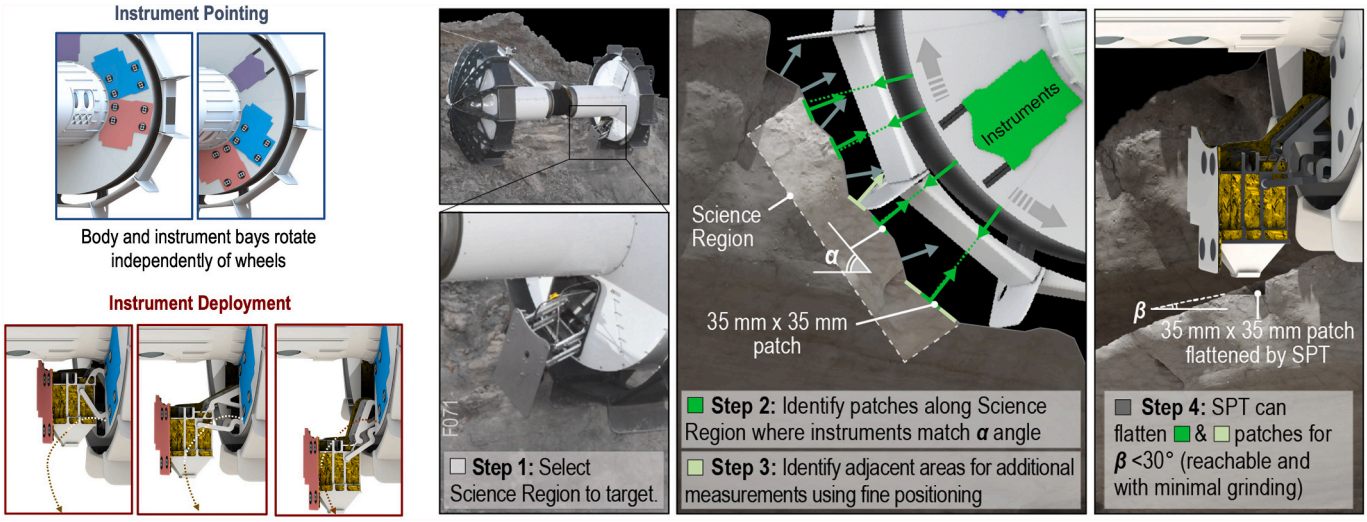

Fig. 11. The Axel System consists of the Axel rover, the instrument payload, the tether and a lander-mounted interface box.

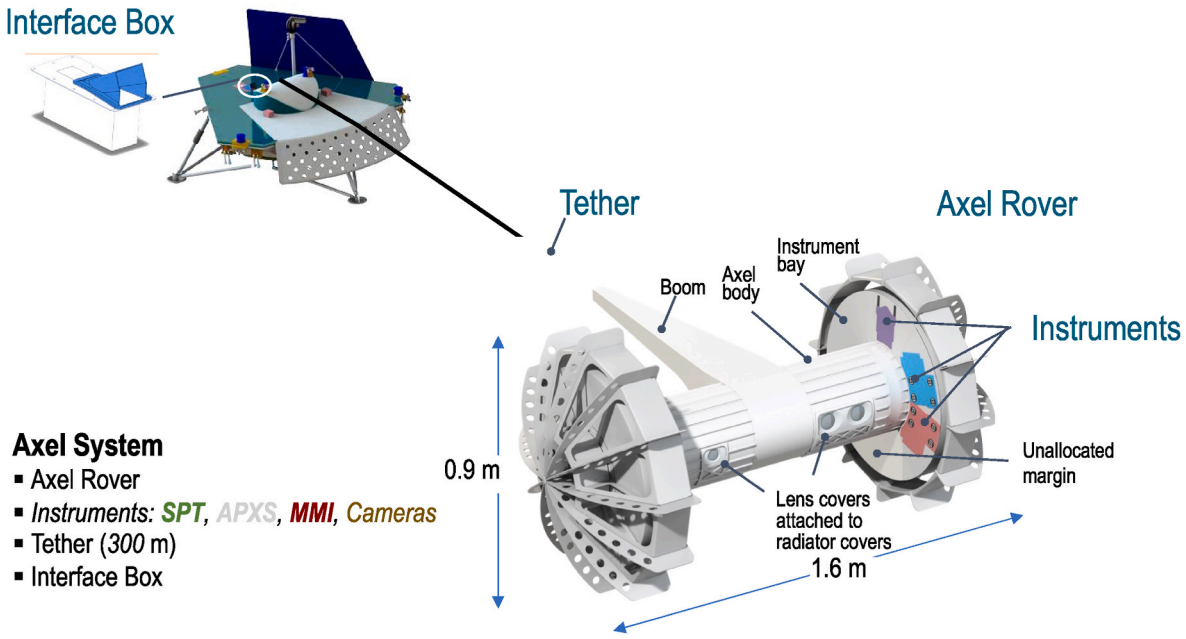

Fig. 12. Preparing a target for measurements follows a step-by-step procedure. The mechanism's long travel facilitates operation on rocky surfaces.

system, such as the one developed and fielded by Brown et al. [37] would not be necessary for this application. A more minimal design that maintains the unspooled tether and provides tether tension sensing (similar to the original Axel design) should suffice. The enclosure over the cable drum protects the tether from dust and debris, and it also insulates the cable from the environment.

6.2. Surface operations

The surface mission timeline is a single lunar daytime (14 Earth days), which includes commissioning, egressing, traversing at most 110 m to reach the pit funnel, descending into the funnel, and rappelling. Along that route, the rover stops at 22 science sites to acquire context imagery and science measurements. At each science site, a canonical set of activities is conducted. Fig. 14 shows a template for these planned operations of the instruments and rover along with parallel ground activities. At each site, 3 h are allocated for positioning the rover, grinding the rock to prepare the surface, and acquiring MMI and APXS measurements. In addition, an additional 1.3 h are allocated as contingency time for science at each site. Combined with 8 contingency sites included in the surface phase plan, Moon Diver has allocated a total of 100% contingency on timeline for science.

The science sub-phase requires two supporting engineering activities: Axel mobility and heat dissipation. Mobility activities, whether traversing flat ground or rappelling, include near real-time ground operations. Operators view navigation images and command the rover to proceed in increments of <1.5 m at a time. During the heat dissipation activity, operators command the rover to point its radiators to the cold sky and switch to a low power hibernation mode.

Models have been developed for the duration of mobility and heat dissipation activities that include the positions of the sun and the geometry of the traverse route. The timeline adds engineering contingency according to simple rules: (1) double the modeled mobility durations to account for uncertainty in lunar terrain and growth during validation;

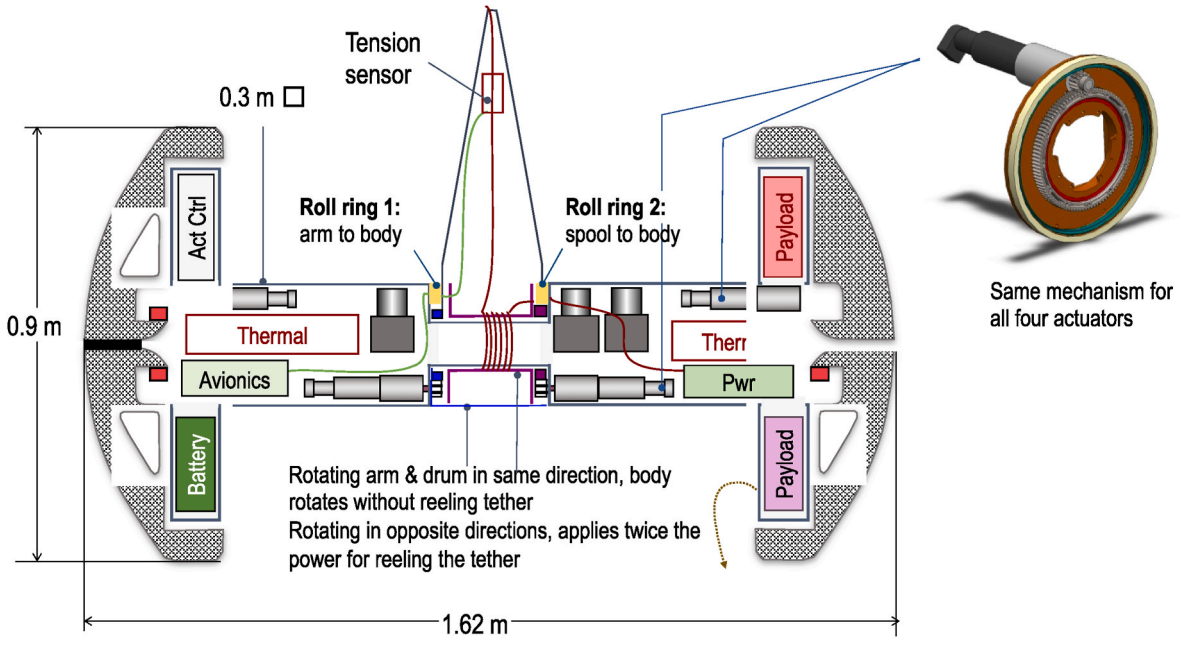

Fig. 13. A cross section of the Axel rover showing the internal architecture.

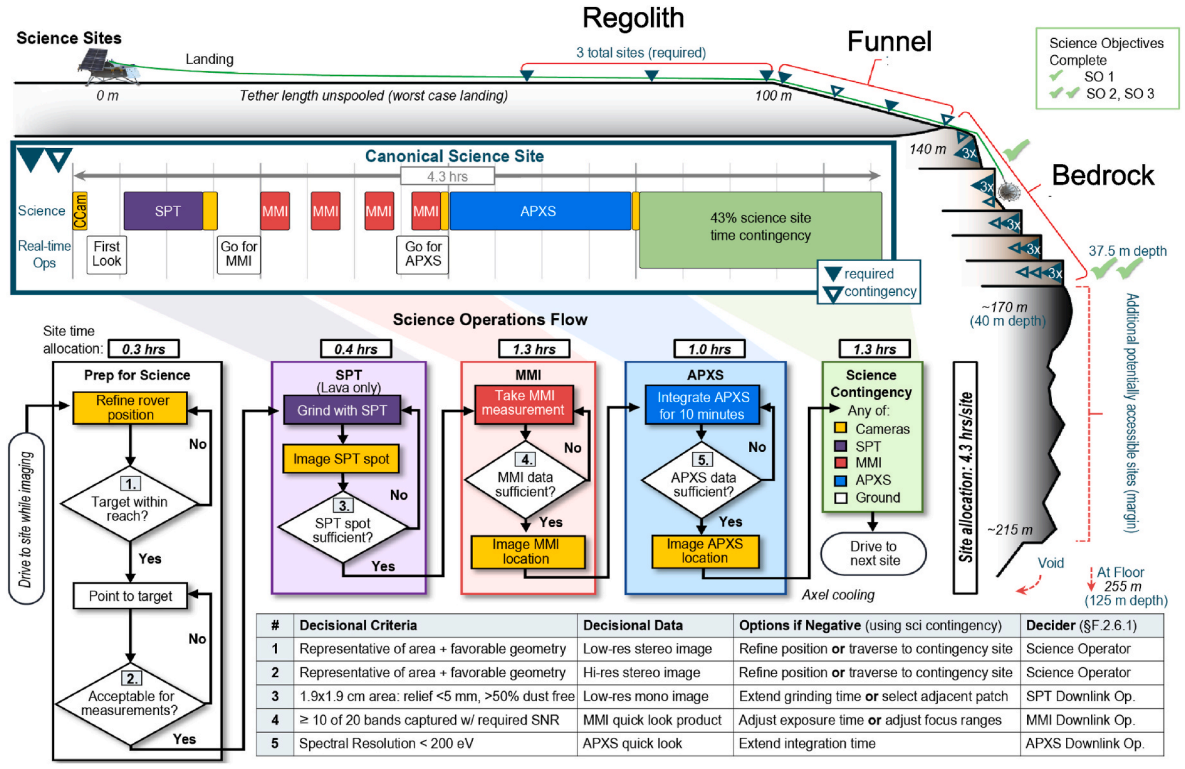

#	Decisional Criteria	Decisional Data	Options if Negative (using sci contingency)	Decider (§F.2.6.1)
1	Representative of area + favorable geometry	Low-res stereo image	Refine position **or** traverse to contingency site	Science Operator
2	Representative of area + favorable geometry	Hi-res stereo image	Refine position **or** traverse to contingency site	Science Operator
3	1.9x1.9 cm area: relief <5 mm, >50% dust free	Low-res mono image	Extend grinding time **or** select adjacent patch	SPT Downlink Op.
4	≥ 10 of 20 bands captured w/ required SNR	MMI quick look product	Adjust exposure time **or** adjust focus ranges	MMI Downlink Op.
5	Spectral Resolution < 200 eV	APXS quick look	Extend integration time	APXS Downlink Op.

Fig. 14. Moon Diver repeats a canonical set of activities at each contact science site. Human-in-the-loop operators confirm *go/no-go* increments. Operators confirm completion of activities in near real time. Commands are selected from menus of pre-validated options; neither long sequences of commands nor resource-modeling is required.

(2) analyze maximum expected value (MEV) thermal case (higher heat loads and deteriorated radiator performance) and allocate additional heat dissipation time as contingency; and (3) allocate 50% contingency (8 h) to the commissioning sub-phase.

In addition to context imaging, science measurements at rocky sites include surface preparation. For these sites, the SPT grinds a small area by controlling the rover's orientation in a sweeping back and forth motion to remove dust and patina that may be present on the rock wall. This would flatten the surface sufficiently for subsequent measurements. The rover then re-orients its instruments to deploy the MMI and APXS for short and at time long-duration integration.

Table 3 summarizes the science and engineering data products that will be generated by the onboard system and downlinked to the ground.

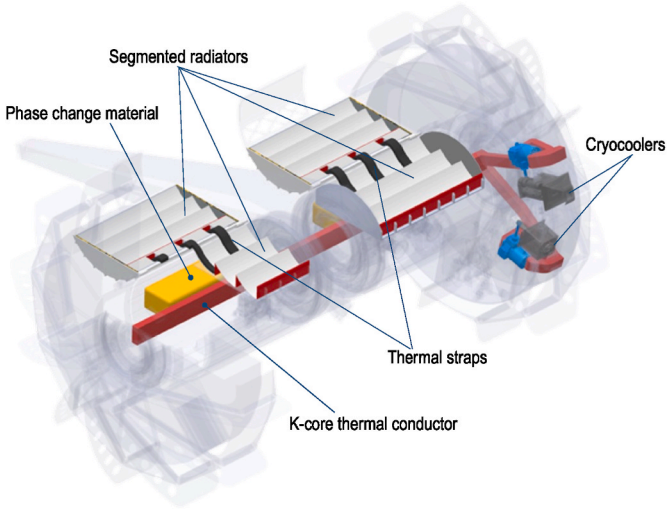

Fig. 15. Axel's thermal design at to accommodate worst-case thermal conditions during the pit excursion.

7. Field campaigns

We conducted a number of field campaigns at different sites using similar scale Axel rovers to the one envisioned for the Moon Diver mission. Tests were conducted: (1) at a rock quarry in Canyon Country, California, (2) in the desert near Black Point Lava Flow in Arizona, (3) at mountainous ranges near JPL, (4) at the basaltic Devolites pit in Arizona, (5) at Golden Queen Mine in the Mojave Desert, California, and (6) at basaltic cliffs of Fossil Falls in Coso range, California [39]. These campaigns used two modes of operation: (1) tele-operation with the operator enjoying a bird's-eye view of the rovers and (2) remote operation using only telemetry from the rover to guide the next actions. The latter tests conducted at sites (4) and (5) simulate operational constraints of the Moon Diver mission concept and those of flight systems.

Fig. 17 shows the Axel rover on three different near-vertical cliffs walls with a height ranging from 15 to 20 m. In 2018, at the Devolites basaltic pit in Arizona, we conducted a field test campaign using an Axel rover prototype with instruments that mimicked Moon Diver's surface-phase science payload: commercial equivalents of the EECAMs that have the same focal plane and optics, a prototype of the microscopic imager, and a commercial-off-the-shelf X-ray Fluorescence from Bruker as a stand-in for the APXS instrument. The science team led realistic mission operations, commanding the rover in near real time and making decisions solely based on telemetry. The rover traversed >100 m,

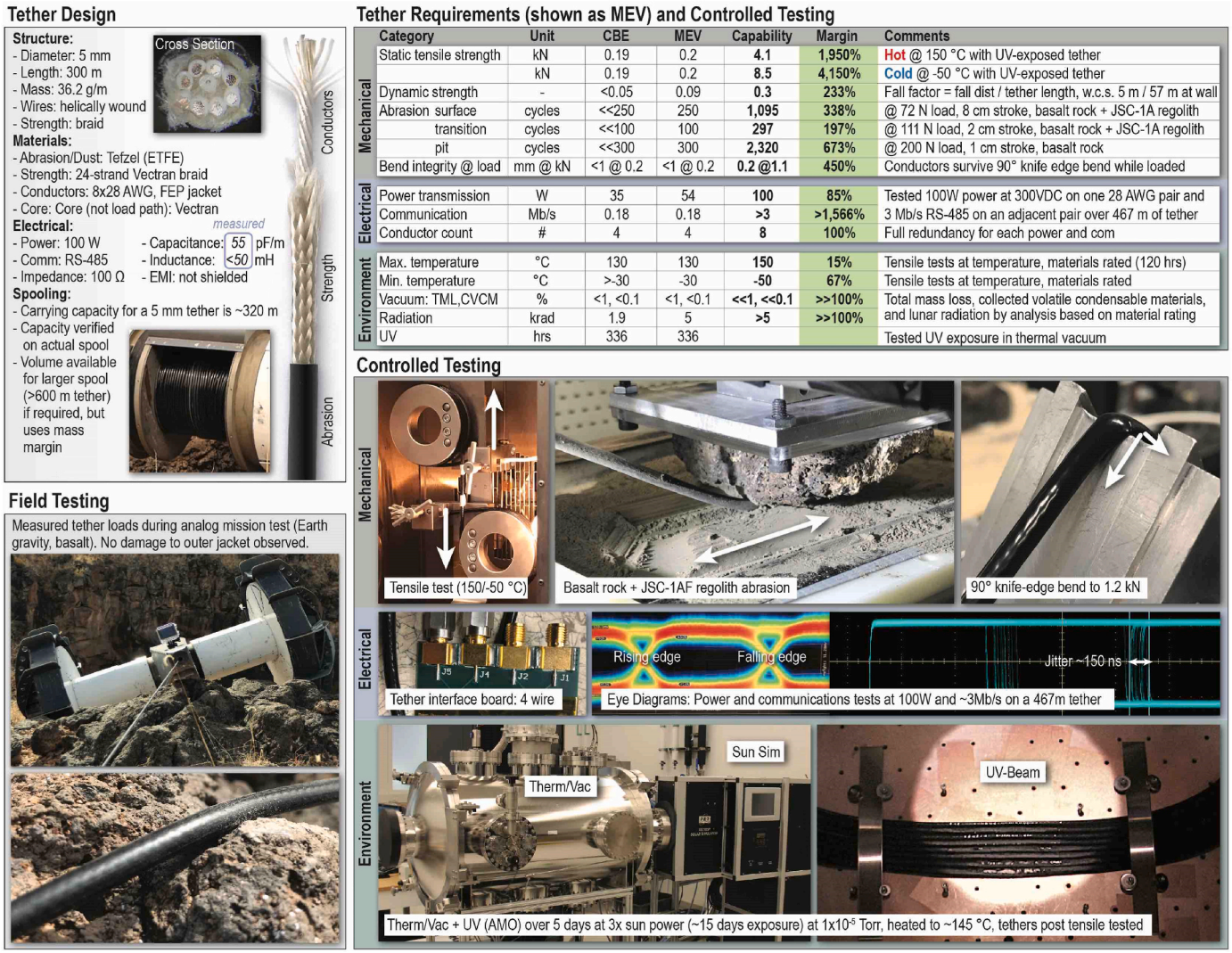

	Category	Unit	CBE	MEV	Capability	Margin	Comments
Mechanical	Static tensile strength	kN	0.19	0.2	**4.1**	**1,950%**	**Hot** @ 150 °C with UV-exposed tether
		kN	0.19	0.2	**8.5**	**4,150%**	**Cold** @ -50 °C with UV-exposed tether
	Dynamic strength	-	<0.05	0.09	**0.3**	**233%**	Fall factor = fall dist / tether length, w.c.s. 5 m / 57 m at wall
	Abrasion surface	cycles	<<250	250	**1,095**	**338%**	@ 72 N load, 8 cm stroke, basalt rock + JSC-1A regolith
	transition	cycles	<<100	100	**297**	**197%**	@ 111 N load, 2 cm stroke, basalt rock + JSC-1A regolith
	pit	cycles	<<300	300	**2,320**	**673%**	@ 200 N load, 1 cm stroke, basalt rock
	Bend integrity @ load	mm @ kN	<1 @ 0.2	<1 @ 0.2	**0.2 @1.1**	**450%**	Conductors survive 90° knife edge bend while loaded
Electrical	Power transmission	W	35	54	**100**	**85%**	Tested 100W power at 300VDC on one 28 AWG pair and
	Communication	Mb/s	0.18	0.18	**>3**	**>1,566%**	3 Mb/s RS-485 on an adjacent pair over 467 m of tether
	Conductor count	#	4	4	**8**	**100%**	Full redundancy for each power and com
Environment	Max. temperature	°C	130	130	**150**	**15%**	Tensile tests at temperature, materials rated (120 hrs)
	Min. temperature	°C	>-30	-30	**-50**	**67%**	Tensile tests at temperature, materials rated
	Vacuum: TML,CVCM	%	<1, <0.1	<1, <0.1	**<<1, <<0.1**	**>>100%**	Total mass loss, collected volatile condensable materials,
	Radiation	krad	1.9	5	**>5**	**>>100%**	and lunar radiation by analysis based on material rating
	UV	hrs	336	336			Tested UV exposure in thermal vacuum

Fig. 16. Results from the tether testing campaign for mechanical, electrical, and environmental properties.

Table 3
Moon Diver's data downlink.

Data Generation	Cameras	MMI	APXS
Required science products	151 image frames	20 image cubes	20 spectra
CBE science data volume	35.6 Gbit	2.5 Gbit	< 0.002 Gbit
Stressing use of science contingency	Additional 88 image frames	Additional 36 image cubes	Additional 36 spectra
MEV science data volume	56.4 Gbit	7.0 Gbit	< 0.005 Gbit
MEV total science data volume	63.4 Gbit (raw)		
MEV engineering data volume	43.4 Gbit (telemetry) 2.5 Gbit (rover nav images)		
Image compression	8 bits/pixel for rover nav & non-decisional science 8 bits/pixel for decisional science images		
Packetization overhead	15% (for tether comm) 15% (for direct-to-Earth link)		
MEV total science + engineering data	109 Gbit (raw) 112 Gbit (compressed and packetized)		
Data downlink by priority	(1) Decisional navigation and science 2% (2) Rover telemetry 26% (3) Lander telemetry 22% (4) Non-decisional science 50%		
Peak Downlink Rates			
Requirement (based on MEV data)	384 kbps		
Capability	768 kbps		
Downlink Rate Margin	**100%**		
Data Latency (downlink duration for decisional navigation & science)			
Requirement (384 kbps)	Rover navigation: stereo 640 × 480 × 8 bpp < **17 s** Sci target selection: stereo 3840 × 1280 × 2 bpp < **68 s**		
Capability (768 kbps)	Rover navigation: stereo 640 × 480 × 8 bpp: **8.5 s** Sci target selection: stereo 3840 × 1280 × 2 bpp: **34 s**		
Data Volume (compressed & packetized)			
Requirement (MEV science and engineering data)	112 Gbit (56 Gbit allocated to science)		
Capability	885 Gbit (790 Gbit allocated to science)		

transitioned from the flat surface to the funnel with a slope of 22°–25° while navigating around obstacles, and rappelled down rocky slopes to reach the vertical pit wall. During these tests, the anchor experienced tensions that reached 400 N with the tether contacting the surface and funnel at a few discrete locations. Due to limited battery life, portions of the traverse used line-of-sight operations to speed up the return of the rover but the rover was able to overcome challenging transitions between the funnel and the wall. Note, however, that ascending is not required for the Moon Diver mission.

At other sites, Axel demonstrated rappelling on mixtures of regolith/rock and across overhangs. Field campaigns in Canyon Country, CA, tested Axel descending a 20-m slope (18 m vertical height) of 65°–85° multiple times, at a top speed of 10 cm/s, where Axel completed a 20-m ascent in approximately 4 min. During some portions of the traverse, rocky debris cascaded onto Axel without causing damage to the rover. By controlling the body pitch as it ascended the cliff, the rover effectively protected its cameras from the falling debris.

During the Arizona desert field test, we conducted experiments to measure the placement repeatability of multiple instruments on a given target at slopes ranging between 60° and 78°. During these maneuvers, we observed no visible slip of the rover despite the fact that all four actuators were rotating simultaneously to reorient the body. The precision of instrument pointing was on the order of ~ 2 mm, was significantly better than our science-driven requirement of <6 mm.

At the JPL Mars Yard and in other field campaigns, we conducted "flip-over" tests. We verified the robustness of Axel's design and operations to such conditions. In the Mars Yard test, we drove the tethered rover up a groomed terrain where one side had a shallow grade that ran parallel to a steep grade incline. This artificially generated terrain was used to induce a tip-over. As Axel drove up the terrain, straddling the two slopes, one wheel began to rise higher than the other. We continued the ascent until the right wheel flipped over the left wheel and landed on the ground, leaving Axel in an upside-down configuration. The rover is designed to handle such maneuvers and survived the impact without damage and continued to ascend successfully under its own power.

In summary, we conducted around a dozen major traverses with Axel across various terrain types and successfully collected a large volume of data both from Axel's own instruments and the tether tension sensor. These experiments showcased Axel's ability to navigate challenging terrain and demonstrated end-to-end operational scenarios of the Axel rovers: traversing to a cliff edge, rappelling, measuring, and ascending. Instruments were placed on targets within 2 mm of one another on a 50° slope [31,32]. Egress and grinding (with SPT) have also been demonstrated at the system level but in separate experiments (see Fig. 18). Videos from Axel field tests are available at [39].

The Axel rover prototype has clocked over a kilometer of mobility in field tests in California and Arizona and has traversed near vertical slopes.

8. Summary and future work

The Moon Diver mission concept takes advantage of the discovery of a natural pit that exposes a deep cross-section of lunar stratigraphy and two advances in capabilities: pinpoint landing and extreme terrain mobility to conduct a science investigation that would deepen our understanding of fundamental processes for differentiation and secondary crusts on the Moon, and to use this knowledge as a keystone for understanding the same processes across the Solar System. It would provide the first *in-situ* observations of a volcanic bedrock sequence on a single-plate planet. Using the rover's instrument suite, we would learn about context, mineralogy, and elemental composition to understand the composition, emplacement, and regolith formation of these secondary crusts.

Fig. 17. Axel has been field tested many times: (left) basalt wall, Devolites, AZ in 2018, (middle) rocky/regolith wall, Canyon Country, CA in 2012, (right) basalt wall at Fossil Falls in the Coso Range, CA in 2019.

Fig. 18. Prototype of the SPT grinding a basaltic rock on a vertical wall using the Axel rover. (*top left):* basaltic rock with laser-rastered patina; (*top right)* fresh and flat after 15 min of SPT operation at 12 W and 5-N preload; *(bottom)* SPT's performance verified in a worst-case geometric configuration: only one wheel grouser in contact on a vertical wall.

Future work will investigate the uncertainty associated with these reconstructed surfaces and modeling the interaction between the rover and the wall, in particular, when transitioning between contact and free hanging. We will use both field experiments and dynamic simulations to inform our investigation. Future work would test mechanisms and seals under lunar conditions that simulate the interaction of a rappelling rover on a collapsed lunar pit. It will also refine the thermal models, investigate edge cases, and environmentally test coupon-sized optical/thermal surfaces with lunar simulants to validate model assumptions (e.g., specularity degradation).

The Moon Diver mission concept is enabled by pinpoint landing and rappelling tethered mobility. It provides a well-margined mission that will provide information regarding the formation of lunar secondary crust, informing the surface formation of terrestrial planets.

Declaration of competing interest

The authors declare that they have no known competing financial interests or personal relationships that could have appeared to influence the work reported in this paper.

Acknowledgements

The work was done at the Jet Propulsion Laboratory, California Institute of Technology, under contract to the National Aeronautics and Space Administration. The information presented about the Moon Diver mission concept is pre-decisional and is provided for planning and discussion purposes only. We would like to express our deep gratitude to the entire 2019 Moon Diver proposal development team including: Matthew Heverly, Jacek Sawoniewicz, Christopher Yahnker, Torkom Pailevanian, Ian McKinley, Bryant Gaume, Catherine Elder, Kyle Uckert, Paul Briggs, Mar Vaquero from the Jet Propulsion Laboratory; John Ricks, and Emily Kloska from Lockheed Martin Space. We would also like to thank the entire Moon Diver science team and especially the science co-investigators: Tony Colaprete of NASA Ames Research Center, Lauren Jozwiak, Rachel Klima, and Angela Stickle from John Hopkins Applied Physics Laboratory, Jennifer L. Whitten and Colin Jackson from Tulane University, Laszlo Keszthelyi from the US Geological Survey, Junichi Haruyama from JAXA/ISAS, Christopher Hamilton from the University of Arizona, Carlé Pieters and James W. Head III from Brown University, Lionel Wilson from Lancaster University, Carolyn Parcheta from Hawaii Volcano Observatory, Debra Needham from NASA Marshall Space Flight Center, Tabb Prissel from NASA Johnson Space Center, Chip Shearer from the Univesrity of New Mexico, Ralph Gellert from University of Guelph, Kate Burgess from the U.S. Naval Research Laboratory, Katie Joy from the University of Manchester, Scott VanBommel from Washington University in St. Louis, James Ashley and Robert Anderson from the Jet Propulsion Laboratory, Peter Isaacson from the Aerospace Corporation, and Kerri Donaldson Hanna from the University of Central Florida.

References

[1] S.R. Taylor, Growth of planetary crusts, Tectonophysics 161 (1989) 147–156.
[2] J.W. Head III, L. Wilson, Generation, ascent and eruption of magma on the Moon: new insights into source depths, magma supply, intrusions and effusive/explosive eruptions (part 2: observations), Icarus 283 (2017) 176–223, https://doi.org/10.1016/j.icarus.2016.05.031.
[3] L. Wilson, J.W. Head III, Generation, ascent and eruption of magma on the Moon: new insights into source depths, magma supply, intrusions and effusive/explosive eruptions (Part 1: theory), Icarus 283 (2017) 146–175, https://doi.org/10.1016/j.icarus.2015.12.039.
[4] L. Wilson, J.W. Head III, Eruption of magmatic foams on the Moon: formation in the waning stages of dike emplacement events as an explanation of "irregular mare patches", J. Volcanol. Geoth. Res. 335 (2017) 113–127, https://doi.org/10.1016/j.jvolgeores.2017.02.009.
[5] L. Wilson, J.W. Head III, Controls on lunar basaltic volcanic eruption structure and morphology: gas release patterns in sequential eruption phases, Geophys. Res. Lett. 45 (2018) 5852–5859, https://doi.org/10.1029/2018GL078327.
[6] J. Haruyama, K. Hioki, M. Shirao, T. Morota, H. Hiesinger, C.H. van der Bogert, H. Miyamoto, et al., Possible lunar lava tube skylight observed by SELENE cameras, Geophys. Res. Lett. 36 (21) (2009).
[7] M.S. Robinson, J.W. Ashley, A.K. Boyd, R.V. Wagner, E.J. Speyerer, B.R. Hawke, H. Hiesinger, C.H. van der Bogert, Confirmation of sublunarean voids and thin layering in mare deposits, Planet. Space Sci. 69 (1) (2012) 18–27.
[8] R.V. Wagner, M.S. Robinson, Distribution, formation mechanisms, and significance of lunar pits, Icarus 237 (2014) 52–60.
[9] http://lroc.sese.asu.edu/posts/202. (Accessed 14 May 2023).
[10] "MoonRise" (PDF). NASA Facts. NASA. June 2010. Archived from the original (PDF) on 16 May 2011.
[11] R.V. Wagner, M.S. Robinson, Lunar pit morphology: implications for exploration, J. Geophys. Res.: Planets (2022), e2022JE007328.
[12] M.I. Staid, C.M. Pieters, J.W. Head III, Mare Tranquillitatis: basalt emplacement history and relation to lunar samples, J. Geophys. Res.: Planets 101 (E10) (1996) 23213–23228.
[13] F. Hörz, F. Lava tubes-potential shelters for habitats, in: *Lunar Bases and Space Activities of the 21st Century*, 1985, pp. 405–412.
[14] I.A. Nesnas, , et al.Moon Diver, A Discovery Mission Concept for Understanding the History of Secondary Crusts through the Exploration of a Lunar Mare Pit, IEEE Aerospace Conference, 2019, pp. 1–23, https://doi.org/10.1109/AERO.2019.8741788.
[15] Y. Cheng, A. Ansar, A. Johnson, Making an onboard reference map from MRO/CTX imagery for Mars 2020 lander vision system, Earth Space Sci. 8.8 (2021), e2020EA001560.
[16] R.V. Wagner, S.K. Rowland, M.S. Robinson, Lunar pits and Hawaiian analogs, in: 49th Lunar and Planetary Science Conference, vol. 2083, 2018, p. 1538.
[17] T. Horvath, P.O. Hayne, D.A. Paige, Thermal and illumination environments of lunar pits and caves: models and observations from the diviner lunar radiometer experiment, Geophys. Res. Lett. 49 (14) (2022), e2022GL099710.
[18] A. Mallik, T. Ejaz, S. Shcheka, G. Garapic, A petrologic study on the effect of mantle overturn: implications for evolution of the lunar interior, Geochem. Cosmochim. Acta 250 (2019) 238–250.
[19] J.W. Head, L. Wilson, Lunar mare volcanism: stratigraphy, eruption conditions, and the evolution of secondary crusts, Geochem. Cosmochim. Acta 55 (1992) 2155–2175.
[20] A. Harris, J. Dehn, S. Calvari, Lava effusion rate definition and measurement: a review, Bull. Volcanol. 70 (2007) 1–22.
[21] L. Keszthelyi, S. Self, T. Thorvaldur, Flood lavas on Earth, io, and Mars, J. Geol. Soc. 163 (2006) 253–264.
[22] J.N. Maki, C.M. McKinney, R.G. Sellar, R.G. Willson, D.S. Copley-Woods, D. C. Gruel, D.L. Nuding, M. Valvo, T. Goodsall, J. McGuire, J. Kempenaar, T. E. Litwin, Enhanced engineering cameras (EECAMs) for the Mars 2020 rover, in: 3rd International Workshop on Instrumentation for Planetary Missions, Abs, 2016, p. 4132.
[23] R. Gellert, R. Rieder, J. Bruckner, B.C. Clark, G. Dreibus, G. Klingelhofer, G. Lugmair, D.W. Ming, H. Wanke, A. Yen, J. Zipfel, S.W. Squyres, Alpha particle X-ray spectrometer (APXS): results from gusev crater and calibration report, J. Geophys. Res. 111 (2006).

[24] R. Rieder, H. Wänke, T. Economou, A. Turkevich, Determination of the chemical composition of Martian soil and rocks: the alpha proton X ray spectrometer, J. Geophys. Res.: Planets 102 (E2) (1997) 4027–4044.
[25] R. Gellert, B.C. Clark, III, and the MSL and MER science teams, in situ compositional measurements of rocks and soils with the alpha particle X-ray spectrometer on NASA's Mars rovers, in: Elements, International Magazine of Mineralogy, Geochemistry, and Petrology, 11, 2015, pp. 39–44.
[26] R.G. Sellar, J.D. Farmer, P. Gardner, P. Staten, A. Kieta, J. Huang, Improved Spectrometric Capabilities for In-Situ Microscopic Imagers, in: Seventh International Conference on Mars, 2007, p. 3017.
[27] R.G. Sellar, J.D. Farmer, J.I. Núñez, Multispectral Microscopic Imager: Petrography on Mars with a Compact, Contact Instrument, in: Concepts and Approaches for Mars Exploration, 2012, p. 4275.
[28] R.G. Sellar, K. Donaldson-Hanna, L. Kerber, Multispectral Microscopic Imager (MMI) for Lunar Surface Missions, in: Lunar Petrology and Landed Instruments Interchange Workshop, 2022. Pasadena, CA.
[29] A.E. Johnson, S.B. Aaron, H. Ansari, C. Bergh, H. Bourdu, J. Butler, J. Chang, R. Cheng, Y. Cheng, K. Clark, D. Clouse, R. Donnelly, K. Gostelow, W. Jay, M. Jordan, S. Mohan, J. Montgomery, J. Morrison, S. Schroeder, B. Shenker, G. Sun, N. Trawny, C. Umsted, G. Vaughan, M. Ravine, J. Schaffner, J. Shamah, J. Zheng, Mars 2020 lander vision system flight performance, AIAA 2022-1214, AIAA SCITECH 2022 Forum (2022), pp 1214–1234.
[30] I.A. Nesnas, P. Abad-Manterola, J.A. Edlund, J.W. Burdick, Axel mobility platform for steep terrain excursions and sampling on planetary surfaces, in: Proceedings of IEEE Aerospace Conference, Big Sky, MT, 2007.
[31] P. Abad-Manterola, J.A. Edlund, J.W. Burdick, A. Wu, T. Oliver, I.A. Nesnas, J. Ceceva, Axel: a minimalist tethered rover for exploration of extreme planetary terrains, IEEE Robot. Autom. Mag. 16 (4) (2009) 44–52.
[32] I.A. Nesnas, J. Matthews, P. Abad-Manterola, J.W. Burdick, J. Edlund, J. Morrison, R. Peters, M. Tanner, R. Miyake, B. Solish, Axel and DuAxel rovers for the sustainable exploration of extreme terrains, J. Field Robot. 29 (4) (2012) 663–685.
[33] J. Matthews, I.A. Nesnas, On the Design of the Axel and DuAxel Rovers for Extreme Terrain Exploration, IEEE Aerospace Conference, 2012.
[34] P. Abad-Manterola, J.W. Burdick, I.A. > Nesnas, Axel rover paddle wheel design, efficiency, and sinkage on deformable terrain, in: *Proceedings Of IEEE Conference On Robotics And Automation* (ICRA), Anchorage, AK, 2010.
[35] J.I. Rodriguez, H. Tseng, B. Zhang, Thermal control system of the moon mineralogy mapper instrument, SAE Int. J. Aerospace (2008) 376–387.
[36] D.L. Domingue, C.T. Russell (Eds.), The MESSENGER Mission to Mercury, Springer Science & Business Media, 2007.
[37] T. Brown, A. Stefanini, N. Georgiev, J. Sawoniewicz, I.A. Nesnas, Series elastic tether management for rappelling rovers, in: IEEE/RSJ International Conference on Intelligent Robots and Systems, IROS), 2018, pp. 2893–2900.
[38] P. McGarey, T. Nguyen, T. Pailevanian, I.A. Nensas, Design and test of an electromechanical rover tether for the exploration of vertical lunar pits, in: IEEE Aerospace Conference, 2020, pp. 1–10.
[39] Axel Rover Field Campaign in CA and AZ: https://www.youtube.com/watch?v=Ijjo1nW94tY/(accessed May 14, 2023).